Available online at www.sciencedirect.com

SCIENCE DIRECT®

Polymer 46 (2005) 6250–6257

polymer

www.elsevier.com/locate/polymer

Transport properties of electrically conducting nylon 6/foliated graphite nanocomposites

Wengui Weng, Guohua Chen*, Dajun Wu

College of Materials Science and Engineering, Huaqiao University, Quanzhou 362021, China

Received 4 November 2004; received in revised form 15 May 2005; accepted 16 May 2005
Available online 14 June 2005

Abstract

In this work, we analyze the conductivity data of the nylon 6/FG nanocomposites using the normalized percolation equations and the general effective equation. From the interpretations of the derived results, we demonstrate that the microstructure of the nanocomposites can be readily deduced. Taking several factors into account, it turns out that the tunneling mechanism should be responsible for the observed non-universality of the critical exponents. Experimental evidences show that the existence of the tunneling conduction should be attributed to the particular structure of the prepared materials.

Keywords: Nylon 6; Graphite; Nanocomposite

1. Introduction

In the proceeding paper [1], we have reported direct fabrication of nylon 6/FG electrically conducting nanocomposites in the presence of foliated graphite (FG) nanosheets. It has been shown that the overall behavior of conductivity as a function of the FG concentration (Fig. 1) could be well described in the framework of percolation theory. The percolation threshold, $\phi_c \approx 0.740$ vol%, could be readily determined from fitting the experimental points to the classical percolation theory Eq. (2)

$$\sigma_m = \sigma_0(\phi - \phi_c)^t \tag{1}$$

This extremely low percolation threshold value could be mainly attributed to the particular geometry of the foliated graphite particles, which possess an average diameter of about 12.1 μm and an average thickness of 51.5 nm. Through the uses of mean-field theory and excluded volume theory correlation of this particle morphology to the percolation threshold could be achieved. However, it should be noted that the percolation Eq. (1) could only be used to describe the conductivity above the critical concentration, while description of the conductivity in the insulating region is beyond its reach. Among the three parameters deduced from Eq. (1) in the previous paper, only the value of ϕ_c have been discussed, interpretations of the values of the non-universal critical exponent t and graphite conductivity σ_0 need more information.

In this article, we would like to interpret the non-universal conductivity behavior of the as-prepared nanocomposites in the first study. We will show that it is possible, through the applications of effective media theories, to make deductions about the particle shapes and spatial distributions in the composites and the microstructure of the nanocomposites. Thus, the critical exponent could be discussed using the currently accepted models for non-universal exponents. Results from further experimental studies devoted to the temperature and electric field effects on the conductivity of the nanocomposites are also to be presented. These evidences then not only identify the transport mechanisms in the FG filled nanocomposites but also satisfactorily explain the theoretically derived parameters.

2. Experimental

Procedures for preparation of nylon 6/FG nanocomposites have been described in detail in the proceeding

---

* Corresponding author. Tel.: +86 595 22692956; fax: +86 595 22692508.
E-mail address: hdcgh@hqu.edu.cn (G. Chen).

0032-3861/$ - see front matter © 2005 Elsevier Ltd. All rights reserved.
doi:10.1016/j.polymer.2005.05.071

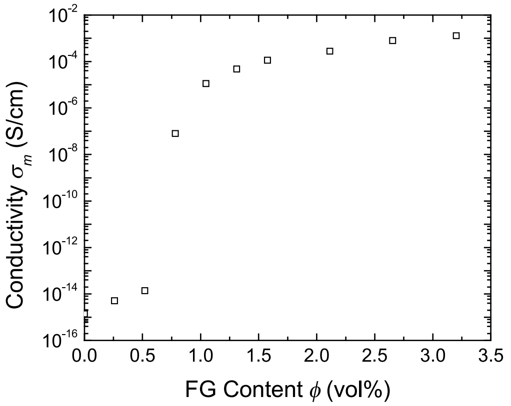

Fig. 1. Electrical conductivities of the nylon 6/FG nanocomposites as a function of FG content.

paper [1]. The data of conductivity as a function of foliated graphite content are the same as those presented in the first study and are re-plotted here in Fig. 1. For measurements of temperature dependency of conductivity, three samples with FG contents of 4.00, 5.00, 6.00 wt% were selected from the series made in the first study. Samples were held between electrodes connected to a DT9205A multimeter, and conductive paste was used to achieve good electrical contact. The conductivity data were measured both at room temperature (25 °C) and at the temperature of liquid nitrogen. While for measurements of electric field dependencies of conductivity samples of various FG contents above but not far from the percolation threshold were newly prepared according to the same procedures. In these measurements, the four-probe method was applied to the whole set of the specimens. Two copper wires were attached to each of the two opposite circular surfaces using conductive paste. An YJ78 DC standard voltage generator was used as the voltage source. To minimize the Joule heating, the effective current passing through the specimens was recorded immediately after a voltage was applied. The current and voltage were collected with two DT9205A multimeters. All the measurements were performed at 25 °C and a relative humidity of 60%. In these two cases, the samples are all disks of 20 mm in diameter and 2.0 mm in thickness, with faces polished with 800-grit sandpaper. That is to say, only the axial conductivity was measured in these temperature and electric field dependency cases.

3. Results and discussion

3.1. Normalized percolation equations

As mentioned above, Eq. (1) is valid only at concentrations above the percolation threshold. In order to interpret the conductivity behaviors of the mixture of conducting and insulating components before and after the critical transition, one should use the following normalized percolation equations (NPE) [2],

$$\sigma_m = \sigma_h \left(\frac{\phi - \phi_c}{1 - \phi_c} \right)^t, \quad \phi > \phi_c \tag{2a}$$

$$\sigma_m = \sigma_l \left(\frac{\phi_c - \phi}{\phi_c} \right)^{-s}, \quad \phi_c < \phi \tag{2b}$$

Here ϕ is the volume fraction of the conducting component and ϕ_c is the percolation threshold or the critical concentration. The exponents t and s characterize the conductivity in the conducting and insulating regions, respectively. These equations give σ_h when $\phi = 1$ and σ_l when $\phi = 0$, so that they can, in principle, fit data in the range $0 < \phi < 1$. However, they cannot apply in the cross-over region [3]:

$$\phi_c - (\sigma_l/\sigma_h)^{1/(t+s)} < \phi < \phi_c + (\sigma_l/\sigma_h)^{1/(t+s)}$$

The conductivity data shown in Fig. 1 thus are fitted simultaneously using equations in Eq. (2), with σ_h, t, s and a single value of ϕ_c as adjustable parameters, while σ_l, the conductivity of nylon 6 in this case, is fixed at 1.385×10^{-15} S/cm, the experimentally measured value for nylon 6 corresponding to the nanocomposite with an FG fraction of 0.00%. The results of these fits are plotted in Fig. 2(a) and (b). The best fitted values of σ_h, t, s and ϕ_c used to plot the

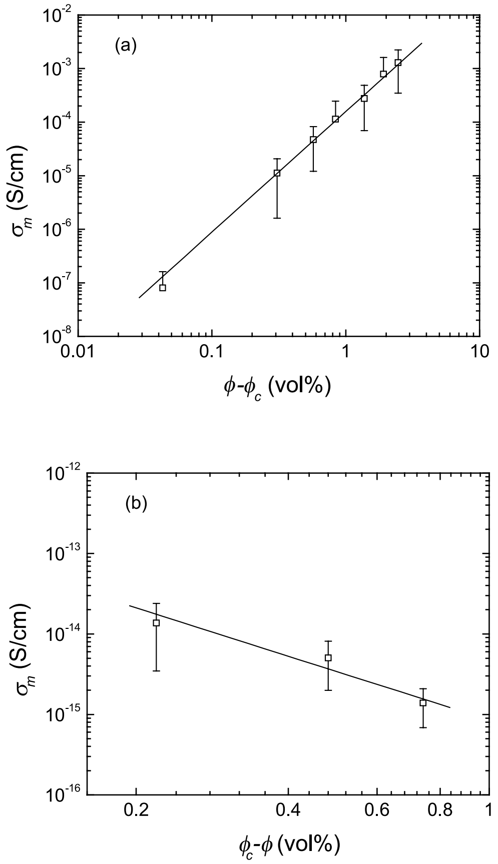

Fig. 2. Plots of the conductivity σ_m as a function of (a) $(\phi - \phi_c)$ and (b) $(\phi_c - \phi)$.

theoretical curves are tabulated in Table 1, together with the statistical uncertainties. As being well demonstrated, simultaneous fitting of the data on either side of ϕ_c to Eq. (2) could eliminate the problem of getting nearly equally good statistical fits for different combinations of ϕ_c and t [4]. Thus, the values of the derived parameters listed in Table 1 should be the best statistical fits, within the error limits. From Table 1, it is seen that the values of σ_h, t and ϕ_c are nearly identical to those obtained using Eq. (1) in the first study [1]. However, it should be recalled that the values of t and s obtained here are clearly higher than the most widely accepted universal ones, $s_{un} \approx 0.87$ and $t_{un} \approx 2.0$, in three dimensions [2]. These results again indicate that the conduction behaviors in the nylon 6/FG nanocomposites should be non-universal. Therefore, it is necessary to give discussions on this issue in order to have a clear understanding on the nanocomposites. We will return to this later.

3.2. General effective media equation

Strictly speaking, percolation theory only applies when either the conductivity or the resistivity of one of the constituent phases is zero. However, in real continuum systems, the ratio of the conductivities is usually not high enough for accurate application of percolation theory. When the ratio of the conductivities of the binary disordered systems is not very small, the conducting behavior of the continuum media could be better accounted by effective media theories (EMT) [5], which assume that each grain of a binary (or higher) system is, on average, surrounded by a mixture possessing the effective conductivity of the composite medium. As far as our nylon 6/FG nanocomposites are concerned, neither the so-called Bruggeman's symmetric medium nor the Bruggeman's asymmetric medium is a realistic model, since their morphologies might lie between these two extremes. Thus, a suitable semi-phenomenological formula developed by McLachlan [6] can be used for these materials. This expression known as general effective media (GEM) equation may be written as

$$\frac{(1-\phi)\left(\sigma_l^{1/t}-\sigma_m^{1/t}\right)}{\sigma_l^{1/t}+A\sigma_m^{1/t}}+\frac{\phi\left(\sigma_h^{1/t}-\sigma_m^{1/t}\right)}{\sigma_h^{1/t}+A\sigma_m^{1/t}}=0 \tag{3}$$

with $A=\dfrac{(1-\phi_c)}{\phi_c}$

Table 1
Adjustable parameters derived from fit of Eq. (2) to the conductivity data presented in Fig. 1

Parameter	Fitted value
σ_h (S/cm)	6.92 ± 1.44
t	2.32 ± 0.07
s	1.90 ± 0.09
ϕ_c (vol%)	0.740 ± 0.049

where σ_m, σ_l and σ_h are the conductivities of the medium, the low- and high-conductivity components, respectively. ϕ is the volume fraction of the high-conductivity component (foliated graphite in this case) and ϕ_c is the critical concentration (i.e. percolation threshold) as defined before. t is an exponent related both to the percolation threshold and the shapes of the grains making up the medium. In certain limits Eq. (2) reduces to the Bruggeman's symmetric and asymmetric medium theories. When $\sigma_l = 0$ or $\sigma_h = \infty$ and $0 < \phi_c < 1$, it has the mathematical form of the percolation Eq. (2). This allows the following relations to be derived, which gives

$$t=\frac{1-\phi_c}{1-L_l}=\frac{\phi_c}{L_h}=\frac{1}{1-L_l+L_h} \tag{4a}$$

for oriented ellipsoids, and

$$t=m_l(1-\phi_c)=m_h\phi_c=\frac{m_l m_h}{m_l+m_h} \tag{4b}$$

for randomly oriented ellipsoids,

where L_l and L_h are coefficients denote the effective demagnetization (depolarization) factors for oriented low- and high-conductivity grains in the direction of current flow [6,7]. The parameters m_l and m_h are values calculable within the limits of σ_l tending to zero and σ_h tending to infinity, respectively, [8]. These four new coefficients are taken as microstructural parameters. Thus, Eq. (4) can, in principle, be used to make deductions about the particle shapes and spatial distributions in composites.

The GEM equation is applicable to the entire range of compositions, besides the results in the cross-over region. It has been demonstrated to be very powerful and suitable for many systems [6,9]. Now, we intend to apply this equation to our experimental results. In practice, the least-squares fitting was carried out with three variable parameters such that the conductivity of foliated graphite σ_h, the critical volume fraction of FG ϕ_c and the exponent t. While the conductivity of the nylon 6, σ_l, is fixed at 1.385×10^{-15} S/cm. After this three-parameter fit, the GEM equation gives the solid line shown in Fig. 3. The adjustable parameters and the corresponding coefficients derived from equations in Eq. (4) are summarized in Table 2. Within the uncertainties of these fitted parameters, it is found that the values of σ_h, t and ϕ_c are very close to those obtained by means of percolation equations.

From Fig. 3 it is seen that the theoretical line excellently agrees with the experimental points. This actually is an encouraging result. Although the overall predication capability of the generalized effective medium theory is yet to be justified, the advantage of the GEM equation used as a fitting model over the percolation conductivity Eq. (1) is evident. In the following sections we will focus our discussions on problems such that, whether there is a clear correlation between the free parameters in the GEM

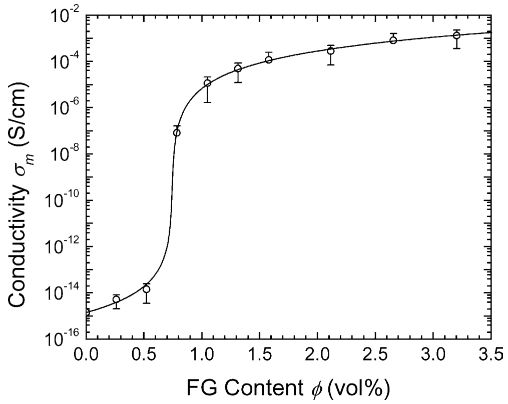

Fig. 3. Electrical conductivities of the nylon 6/FG nanocomposites as a function of FG content. The solid line is the fit of the experimental data to the GEM Eq. (3).

equation and whether the microstructural parameters could be used in deductions of grain morphologies and spatial distributions. The non-universality of the critical exponent t and the conductivity of foliated graphite σ_h need separate discussions.

3.3. Derivation of grain morphologies and spatial distributions from EMT

As argued by numerous authors [10,11], $L_h \to 0$ (i.e. $m_h \to \infty$) means that the current completely avoids the insulating grains and always tries to remain in a continuous conducting sponge. Indeed, the bound $L_h = 0$ corresponds to an asymmetric medium in which insulating grains are coated by the conducting component; in such a case the critical volume fraction for the conducting phase to percolate is $\phi_c = 0$. Previous investigations on the carbon black and flexible epoxy system suggested that the low value of L_h for the conducting grains implies that the system can be described either with the Malliaris and Turner [12] or Kusy [13] models, in which the conducting grains coat the insulating ones, or with the new grain consolidation model proposed by Roberts and Schwartz [14]. In this model the filler particles form conducting lumps and nodes configuration, which has also been supported by the evidence from SEM examination [9]. Hence, since the present materials possess very low values of L_h and ϕ_c, the conductive network formed by foliated graphite nanosheets in the nylon 6/FG nanocomposite can be viewed as a conducting backbone in the binary medium. Besides, since L_h denotes the demagnetization factor associated with the principal axis along which the electric field is impressed, its value is zero for flat disks with their faces or for needles with their axes parallel to the field [7]. The experimental value of L_h thus corresponds to highly flattened ellipsoids, which is consistent with the flaky nature of the foliated graphite particles. Similar results were also obtained for compressed expanded graphite (CEG) [15].

Concerning the low conductivity component, nylon 6 in this case, a high value of the effective demagnetization coefficient L_l corresponds to this component wrapping around or nearly completely coating the conducting particles (foliated graphite grains) [10]. This is realistic for the nylon 6/FG systems. This explanation of the reasonably high values of L_l has also been assumed to be in agreement with the morphology of compressed graphite powders [10]. As for spheres $L_l = 1/3$, the derived value of L_l thus corresponds to ellipsoidal nylon 6 'grains'. Indeed, the value of m_l obtained in this case is consistent with what is to be expected for randomly orientated ellipsoids [16].

Thus, through the use of the above specified theoretical methods and the interpretations of the derived results, together with the experimental evidences obtained in the first study [1], it is now possible to make a clearer visualization of the geometrical structure of the nylon 6/FG nanocomposites. Due to the high aspect ratio of the foliated graphite nanosheets, they are effective in forming conductive networks. Since nylon 6 is a semi-crystalline polymer, it is obvious that the FG particles can only be distributed in the amorphous part of the matrix. Thus the probability for FG nanosheets to contact or overlap is further enhanced, especially when they are dispersed with random orientations. Meanwhile, the nylon 6 can be viewed as filling in the empty volume in the porous FG backbone, which is similar to the structure of 'house of cards'. With the presence of functional oxygen-containing groups on the graphite sheets, a good wetting of the filler by the nylon 6 is possible, accounting for a high L_l value.

Due to the contributing work of Meredith and Tobias [8], calculation of the aspect ratio of the flattened spheroids can be realized by relating the derived microstructure parameters, $m_{h(l)}$ and the depolarization factors $L_{h(l)}$. Indeed, this approach has been successfully applied to the investigation of various carbonaceous materials under compaction [10,15,17]. In dealing with the effective conductance of concentrated suspensions of ellipsoidal particles, Meredith and Tobias [8] derived and gave an expression as

$$1-f=(K_m)^{\beta}\left(\frac{K_m-K_d}{1-K_d}\right)\left(\frac{K_m+\alpha K_d}{1+\alpha K_d}\right)^{\gamma} \tag{5}$$

Table 2
Adjustable parameters (σ_h, t and ϕ_c) obtained from fitting of GEM Eq. (3) to the experimental data shown in Fig. 1, and corresponding coefficients calculated from equations in Eq. (4)

σ_h (S/cm)	t	ϕ_c (vol%)	$L_h \times 1000$	L_l	m_h	m_l
7.49 ± 3.33	2.34 ± 0.12	0.743 ± 0.042	3.17 ± 0.18	0.576 ± 0.022	315 ± 24	2.36 ± 0.12

with f = volume fraction of the dispersed phase

$$K_{\mathrm{m}} = \frac{k_{\mathrm{m}}}{k_{\mathrm{c}}}$$

k_{m}, conductivity of the mixture; k_{c}, conductivity of the continuous phase

$$K_{\mathrm{d}} = \frac{k_{\mathrm{d}}}{k_{\mathrm{c}}}$$

k_{d}, conductivity of the dispersed phase, and

$$\alpha = \frac{2-3L^a}{3L^a+1}$$

$$\beta = 3L^a\left(\frac{1-2L^a}{3L^a-2}\right)$$

$$\gamma = \frac{2(3L^a-1)^2}{(3L^a-2)(3L^a+1)}$$

where L^a is one of the three depolarization factors, $\sum_i L^i = 1$, describing the shape of ellipsoids with semiaxes $a=b\neq c$. Since the parameters m_{h} and m_{l} are defined in the frame of Bruggeman's asymmetric theory [6,16] that

$$\begin{cases} \sigma_{\mathrm{m}} = \sigma_{\mathrm{l}}(1-f)^{-m_{\mathrm{h}}} = \sigma_{\mathrm{l}}(1-\phi)^{-m_{\mathrm{h}}}, \text{ with } f=\phi, \text{ if the dispersed phase is conducting one} \\ \sigma_{\mathrm{m}} = \sigma_{\mathrm{h}}(1-f)^{m_{\mathrm{l}}} = \sigma_{\mathrm{l}}\phi^{m_{\mathrm{l}}}, \text{ with } f=1-\phi, \text{ if the dispersed phase is insulating one} \end{cases} \tag{6}$$

Thus, based on the relation $L^a = L^b = 1/2(1-L^c)$, together with Eqs. 5 and 6 in the limits $k_{\mathrm{d}}=\sigma_{\mathrm{h}}=\infty$ and $k_{\mathrm{d}}=\sigma_{\mathrm{l}}=0$, respectively, m_{h} and m_{l} are derived as

$$\begin{cases} m_{\mathrm{h}} = -\dfrac{1}{\beta} = \dfrac{2-3L_{\mathrm{h}}^a}{3L_{\mathrm{h}}^a(1-2L_{\mathrm{h}}^a)} = \dfrac{1+3L_{\mathrm{h}}^c}{3L_{\mathrm{h}}^c(1-L_{\mathrm{h}}^c)} \\ m_{\mathrm{l}} = \dfrac{1}{\alpha+\beta+\gamma} = \dfrac{3L_{\mathrm{l}}^a+1}{6L_{\mathrm{l}}^a(1-L_{\mathrm{l}}^a)} = \dfrac{5-3L_{\mathrm{l}}^c}{3(1-L_{\mathrm{l}}^{c2})} \end{cases} \tag{7}$$

It is now possible to calculate the aspect ratio of the graphite nanosheets dispersed within the nylon 6 matrix, considering that the graphite sheets are similar to oblate (flattened) spheroids with semiaxes such that $a=b>c$. Then the eccentricity e is linked to the corresponding depolarization factor L^c as

$$\begin{cases} e = \sqrt{\left(\frac{a}{c}\right)^2 - 1} \\ L^c = \dfrac{1+e^2}{e^3}(e - tg^{-1}e) \end{cases} \tag{8}$$

In this case, if $a=b=c$, i.e. corresponding to spheroids, the $e=0$, and $L^{\mathrm{a}}=L^{\mathrm{b}}=L^{\mathrm{c}}=1/3$. Then according to Eq. (7), m_{h} and m_{l} take their minimum values 3 and 3/2, respectively. As the aspect ratio rises, $L^{\mathrm{c}}\to 1$ and $L_{\mathrm{a}}=L_{\mathrm{b}}\to 0$, corresponding to thin disks. Hence, m_{h} and m_{l} both tend to infinity. The values of m_{h} and m_{l} versus the aspect ratio of the grains are shown in Fig. 4.

The aspect ratio value of foliated graphite calculated from Eq. (8) is listed in Table 3. For the sake of comparison, the aspect ratio values derived from other methods are also presented. It is seen that the values derived in the framework of EMT is much higher than those obtained from the experimental measurements, mean-field theory and excluded volume theory which have been discussed previously [1]. Because of this obvious inconsistency, one may have to first take into consideration some of the requirements for the application of EMT [5,6,17].

Firstly, effective media theories consider a medium completely filled with ellipsoids with an infinite range of sizes. In practice, such an extreme situation is never satisfied, even if the particle size distributions of the powders are sometimes broad. In addition, the number of particles must be sufficiently high in order for any given grain to be assumed to be homogeneously surrounded by the medium. As can be observed from the laser counting analyses [1], the size distributions of the foliated graphite are far from what can be called infinite. Although their thickness is in the nanometer range, so that the number of particles may be very high, the requirements of the effective media are still difficult to be met.

Secondly, Eq. (6) is such that the limits $\sigma_{\mathrm{h}}=\infty$ and $\sigma_{\mathrm{l}}=0$ are assumed, and for situations which $\phi_{\mathrm{c}}=1$and $\phi_{\mathrm{c}}=0$ are implied, respectively. Thus, although derivation of the aspect ratio of carbonaceous powders could be well performed in the cases of carbonaceous powders and EG under compaction [15,17], the present nylon 6/FG system is not the case.

Furthermore, derivation and application of Eq. (4b) assume a random orientation of the grains. Owing to the flake morphology of the foliated graphite nanosheets, an orientation of the particles might be expected [1]. Hence, Eqs. (4b), (6) and (7) might not be obeyed fully. Then it is possible that while the GEM can be perfectly applied in

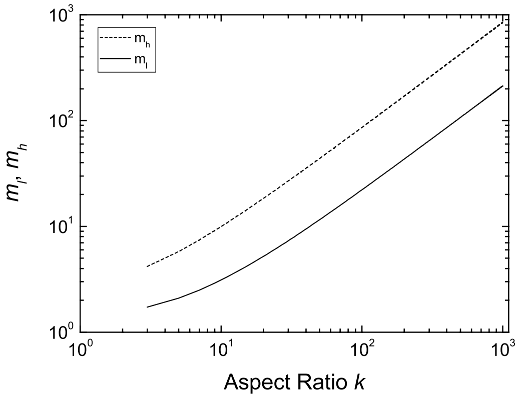

Fig. 4. Morphological parameters m_{h} and m_{l} for high (low) conductivity phases versus the aspect ratio $k=a/c$ of these oblate phases.

Table 3
Values of the aspect ratio derived from various approaches

EMT	MFT	EVT	EXP
370±28	159±11	$154\leq k\leq 239$	235±10

EMT, effective media theories; MFT, mean-field theory; EVT, excluded volume theory; and EXP, experimental [1].

describing the conduction behavior of the composites, the deduced microstructure parameters cannot be used to accurately identify the particle shape of the filling phase.

3.4. The critical exponent and conductivity of the foliated graphite

Now that the structure of the present nanocomposites has been interpreted, it is possible and necessary to carry out separate discussions on the values of the other two parameters, the critical exponent t and the conductivity of the foliated graphite σ_h.

It is apparent from Tables 1 and 2 that the values obtained for the critical exponents, beyond experimental and statistical uncertainties, are larger than the universal ones predicted from computer simulations. From the microstructures just discussed, the structure of the nylon 6/FG system should be described in the frame of continuum percolation, for which there are two features having no counterparts in lattice percolation [18]. The first one is the above-mentioned dependence of percolation threshold on the structure; and the second one is a relation between the critical exponents and the local geometrical properties of the system, that is to say the value of the critical exponents depend on the structure. One origin for the increase in t is the anisotropy of the conductivity. However, in similar systems, Celzard et al. [19] demonstrated that this mechanism could probably be ruled out.

Another consideration is the influence of the existence of the tunneling conduction [20]. From the conductivity figures, it is seen that the conductivity values of the nylon 6/FG nanocomposites approach a limiting conductivity (about 10^{-3} S/cm) in high-concentration domain. Such saturation of conductivity suggests that there might have polymer in the conductive network. Actually, experimental evidence [20] indicates that in carbon black filled polymer composites, even for compounding under high pressure and for concentration greatly higher than the percolation threshold, the conducting aggregates are always separated by thin layers of insulating polymer. As demonstrated by the interpretations of the mircostructural parameters, wrapping of the FG particles by the nylon 6 is possible. In the present case, owing to the oxidation effects during the preparation of the precursor GICs [21–23], some carbon double bonds were oxidized, leading to the presence of oxygen-containing functional groups on foliated graphite [24,25]. This is supposed to facilitate physical and chemical interactions between FG and some polymers (or monomers) [26]. Indeed, during the fabrication of nylon 6/FG nanocomposites, the monomer was found to wet the FG particles very well. This might be due to the particular surface properties of the FG and results in enhanced interactions between the FG and the nylon 6 matrix, which could be supported by our thermal analysis evidences [1,27]. Then upon completion of the in situ polymerization, presence of nylon 6 coatings around the FG grains is quite realistic. The FG particles forming the percolation-like network thus only touch 'electrically' [28]. The measured finite macroscopic conductivity must be attributed to the existence of interparticle tunneling.

3.5. Tunneling conduction

Tunneling conduction is a thermal fluctuation assisted transport process [29]. In this case, the conductivity of a composite can be described by the behavior of a single tunnel junction and expressed, in a first approximation, as

$$\sigma_m = \sigma_c \exp(-2\chi_t d) \tag{9}$$

where σ_m is the composite conductivity, σ_c is a constant and d is the distance between conductive particles. In this expression, $\chi_t = (2mV(T)/\hbar^2)^{1/2}$, where m is the mass of the charge carriers, $V(T)$ is the temperature modified barrier height and $\hbar$ is Planck's constant divided by 2π. This expression can be envisioned as a simple tunneling conductivity in which the increasing temperature induces the energy barrier height to decrease [30]. This is actually supported by our temperature variation data that sample resistances increased by about twenty times when samples were cooled from room temperature to that of liquid nitrogen. If a random distribution of particles is assumed, the mean distance among particles has been shown to be proportional to $\phi^{-1/3}$ [30]. Then if Eq. (9) is valid, drawing $\log \sigma_m$ as a function of $\phi^{-1/3}$ will yield a straight line. Indeed such a linear dependence (Fig. 5) is also observed for our materials in concentrations well above the percolation

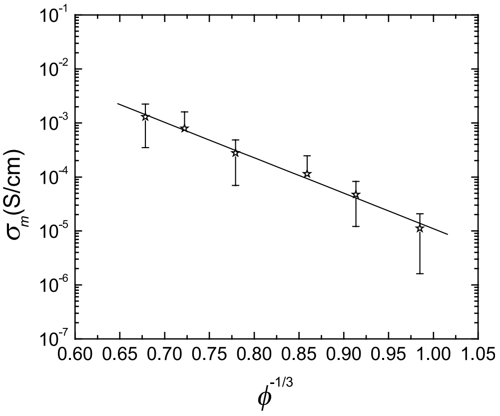

Fig. 5. Variations of σ_m with respect to $\phi^{-1/3}$ for nylon 6/FG nanocomposites with FG content above the percolation threshold.

threshold, in support of Eq. 9. This has also been justified in the polyethylene-graphite composites [30].

In addition, in measurements of electric field dependency of conductivity, all samples of nylon 6/FG nanocomposites were found to exhibit non-linearity in the *I–V* characteristics. Fig. 6 shows in logarithmic scales two typical examples of the *I–V* curves. The curves are current limited within the range of measurements. At sufficiently low voltages (*V*), the curves are linear. With increasing bias, the curves deviate from linearity and bend towards the current (*I*) axis. Furthermore, we have also verified that only under a given low electric field this behavior is reversible.

Previously, a simple formula was proposed to describe the nonlinear conduction in conducting polymer composites [31]. In this formula the current density and the field intensity is related in a power law equation

$$J = \Sigma_0 E^{\beta} \tag{10}$$

where Σ_0 is a constant and β is an exponent greater than unity. Clearly, when the conductive behaviors of the conducting composites are ohmic, the parameter β equals to unity. However, when the conduction in the composites deviates from the linear behavior, β is generally found to increase above 1.

Fig. 7 presents the current density as a function of electric field for nylon 6/FG nanocomposites fitted by Eq. (10). It can be seen that the agreement between the fitted curves and the experimental points is quite good. The more the foliated graphite in the nanocomposite the better the fit is. The values of the constant Σ_0 and the exponent β derived from the computer fitting are plotted in Fig. 8 as a function of foliated graphite content. For comparison the original percolation curve and linear conductivity are also presented in the same plot. From Fig. 8, one can easily read that the exponent β increases from 1.06 at a foliated content of $\phi = 1.950\%$ to 1.55 as the filler fraction approaches the percolation threshold $\phi_c$from above. Meanwhile, the constant Σ_0 increases in almost the same track of the linear conductivity σ_0 versus ϕ. Since the value of the exponent β is an indication of the contribution of the nonlinear mechanisms, one can conclude that the greater the deviation of the exponent β from unit, the greater the non-linearity in the composite.

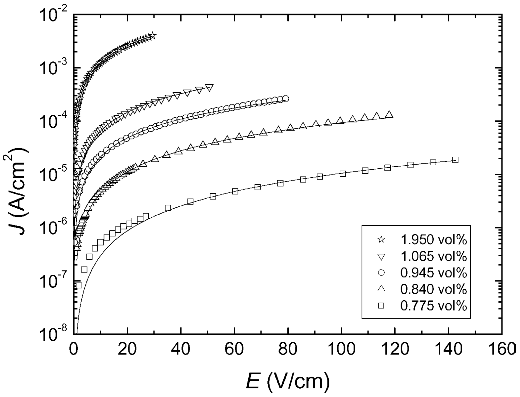

Fig. 7. Fit of the current density (J) as function of electric field intensity (E) to the relation $J = \Sigma_0 E^{\beta}$.

Considering that the foliated graphite in the nylon 6/FG nanocomposites is ohmic, one may expect the tunneling across the thin insulating polymer layers to contribute additional mode of conduction mechanism, besides the usual conduction through conducting graphite, to the conduction of the nanocomposites subjected to higher electric field. Thus, the greater the values of β, the more significant the tunneling conduction in the nanocomposites. As $\phi \rightarrow \phi_c$ from above, both the width and percentage of the insulating polymer layer increase, thus a correlation between the tunneling conduction and the FG content ϕ can also be qualitatively established.

This tunneling mechanism also accounts for the fitted values of the conductivity of the foliated graphite. It is seen from Tables 1 and 2 that the obtained σ_h values are actually far below the value to represent accurately a typical graphite particle, which has a magnitude in the order of 10^4 S/cm [32]. However, it is obvious that if the contacts among graphite particles are of the tunneling type, it will definitely give rise to higher contact resistances.

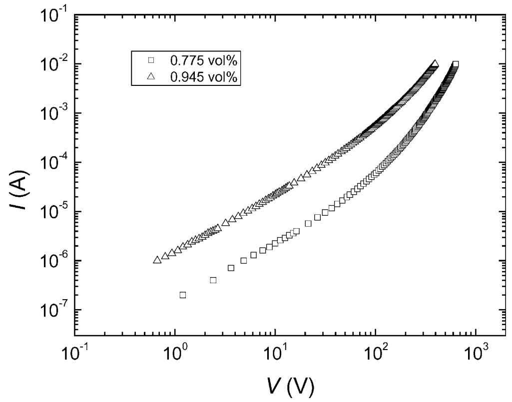

Fig. 6. Two typical nonlinear *I–V* curves of the nylon 6/FG nanocomposites with FG volume content as indicated.

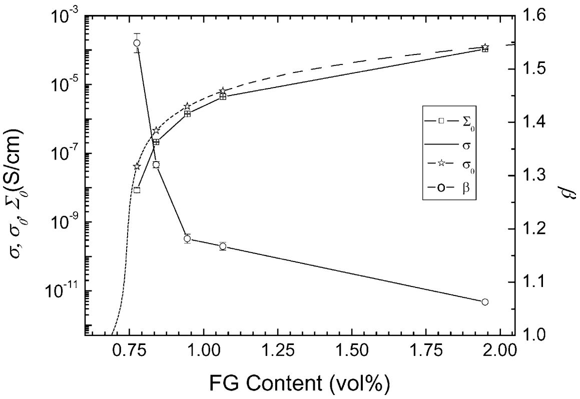

Fig. 8. The exponent β, constant Σ_0, linear conductivity σ_0 and percolation curve of conductivity σ as a function of foliated graphite volume fraction ϕ.

4. Conclusions

By examining the conductivity data of the nylon 6/FG nanocomposites, electrical transport properties in this kind of materials have been studied. The normalized percolation equations could well describe the conductivity of the nanocomposites both above and below the percolation threshold, while the general effective media equation was demonstrated to be more powerful. The GEM equation not only could successfully model the conductivity to the entire range of compositions, but also contains free parameters that could be used to derive information concerning the grain shapes and spatial distributions in composites. Despite that notable deviations of the calculated values of the aspect ratio from the experimental one were observed, the derived microstructural parameters accurately deduce the microstructure of the nanocomposites. It should be the particular structure of the present nanocomposites that results in the non-universality of the critical exponents. Taking several factors that may affect the critical exponent *t* into account, it turned out that the tunneling mechanism should be here responsible for the observed results. Such tunneling conduction could be readily identified by a simple examination of a new dependency of the conductivity on the foliated graphite concentration greater than the percolation threshold. Experimental evidences from the measurements of temperature and electric field dependencies of conductivities also justified that there indeed exists tunneling conduction.

Acknowledgements

The authors would like to thank Prof Zhiyong Lin for supplying the monomer and enjoy helpful discussions with him. Also the help from Dr Jianming Lin, Jianxin Weng, Cuiling Wu and the work of several students are gratefully acknowledged. This work is sponsored by National Natural Science Foundation of China (No. 50373015, 20174012).

References

[1] Weng WG, Chen GH, Wu DJ, Chen X-F, Lu JR, Wang PP. J Polym Sci, Part B: Polym Phys 2004;42:2844.
[2] Stauffer D, Aharony A. Introduction to percolation theory. London: Taylor and Francis; 1991.
[3] Chiteme C, Mclachlan DS. Physica B 2000;279:69.
[4] Wu J, McLachlan DS. Phys Rev B 1997;56:1236.
[5] Landauer R. Electrical transport and optical properties of inhomogeneous media. Am Inst Phys Conf Proc 1978;40:2–43.
[6] Mclachlan DS, Blaszkiewicz M, Newnham RE. J Am Ceram Soc 1990;73:2187.
[7] Sen PN, Scala C, Cohen MH. Geophysics 1981;46:781.
[8] Meredith RE, Tobias CW. Adv Electrochem Electrochem Eng (New York) 1962;2:15.
[9] Deprez N, Mclachlan DS, Sigalas I. Solid State Commun 1988;66:869.
[10] Deprez N, Mclachlan DS. J Phys D: Appl Phys 1988;21:101.
[11] Mclachlan DS. J Phys C 1988;21:1521.
[12] Malliaris A, Turner DT. J Appl Phys 1971;42:614.
[13] Kusy RP. J Appl Phys 1977;48:5301.
[14] Roberts JN, Schwartz LM. Phys Rev B 1985;31:5990.
[15] Celzard A, Mareche JF, Furdin G, Puricelli S. J Phys D: Appl Phys 2000;33:3094.
[16] Mclachlan DS. J Phys C: Solid State Phys 1987;20:865.
[17] Celzard A, Mareche JF, Payot F, Furdin G. Carbon 2002;40:2801.
[18] Kovacik J. Scripta Materialia 1998;39:153.
[19] Celzard A, Mareche JF. Physica A 2003;317:305.
[20] Balberg I. Phys Rev Lett 1987;59:1305.
[21] Chung DDL. J Mater Sci 1987;22:4190.
[22] Furdin G. Fuel 1998;77:479.
[23] Nakajima T, Matsuo Y. Carbon 1994;32:469.
[24] Ramesh P, Sampath S. Anal Chem 2000;72:3369.
[25] Ramesh P, Sampath S. Analyst 2001;126:1872.
[26] Pan YX, Yu ZZ, Ou YC, Hu GH. J Polym Sci, Part B: Polym Phys 2000;38:1626.
[27] Weng W, Chen G, Wu D. Polymer 2003;44:8119.
[28] Rubin Z, Sunshine A, Heaney MB, Bloom I, Balberg I. Phys Rev B 1999;59:12196.
[29] Sheng P, Sichel EK, Gittleman JI. Phys Rev Lett 1978;40:1197.
[30] Ezquerra TA, Kulescza M, Cruz CS, Balta-Calleja FJ. Adv Mater 1990;2:597.
[31] Dechkovskaya K, Yipman T, Dogadkin B. Rubber Chem Technol 1953;26:810.
[32] King JA, Tucker KW, Vogt BD, Weber II E, Quan CL. Polym Compos 1999;20:643.